

# Phase Transitions in the Two-Dimensional $XY$ Model with Random Phases : a Monte Carlo Study.

J. Maucourt, and D.R. Grempel

*CEA/Département de Recherche Fondamentale sur la Matière Condensée.*

*SPSMS, CENG, 17, rue des Martyrs, 38064, Grenoble Cedex 9, France.*

(October 9, 2018)

## Abstract

We study the two-dimensional  $XY$  model with quenched random phases by Monte Carlo simulation and finite-size scaling analysis. We determine the phase diagram of the model and study its critical behavior as a function of disorder and temperature. If the strength of the randomness is less than a critical value,  $\sigma_c$ , the system has a Kosterlitz-Thouless (KT) phase transition from the paramagnetic phase to a state with quasi-long-range order. Our data suggest that the latter exists down to  $T = 0$  in contradiction with theories that predict the appearance of a low-temperature reentrant phase. At the critical disorder  $T_{KT} \rightarrow 0$  and for  $\sigma > \sigma_c$  there is no quasi-ordered phase. At zero temperature there is a phase transition between two different glassy states at  $\sigma_c$ . The functional dependence of the correlation length on  $\sigma$  suggests that this transition corresponds to the disorder-driven unbinding of vortex pairs.

PACS numbers: 75.10.Nr, 75.40.Mg, 74.40

## I. INTRODUCTION

The two-dimensional  $XY$  model with quenched phase disorder describes the thermodynamics of a variety of systems of experimental interest. Examples of these include magnetic systems with random Dzyaloshinskii-Moriya interactions [1], crystal systems on disordered substrates [2], arrays of Josephson junctions with positional disorder [3,4] and vortex glasses [5]. The critical properties of these systems are described by the model Hamiltonian

$$H = -J \sum_{\langle i,j \rangle} \cos(\theta_i - \theta_j - A_{ij}), \quad (1)$$

where the sum runs over the  $N_b$  bonds of a  $2-d$  square lattice,  $\theta_i$  is a phase variable attached to site  $i$  and  $A_{ij} = -A_{ji}$  is a quenched random bond-variable whose precise physical meaning depends on the nature of the system described by the model. We assume for simplicity that the phase shifts on different bonds are uncorrelated and that each configuration  $\{A_{ij}\}$  occurs with probability

$$P[A] = \frac{1}{(2\pi\sigma)^{N_b/2}} \exp \left[ -\frac{1}{2\sigma} \sum_{\langle ij \rangle} A_{ij}^2 \right]. \quad (2)$$

The nature of the phase diagram of this system in the  $\sigma-T$  plane has been controversial. By mapping model (1) into a two-dimensional Coulomb gas in a random background of frozen dipoles, Rubinstein *et al.* [1] generalized the original treatment [6] of the Kosterlitz-Thouless (KT) transition to the random case. Their analysis leads to the phase diagram shown in Fig. 1. For  $\sigma > \sigma_c = \pi/8$  the system is paramagnetic at all temperatures. For  $\sigma < \sigma_c$ , in the limit of infinite vortex core energy, two lines,  $T_{\pm}(\sigma) = \frac{\pi J}{4} [1 \pm \sqrt{1 - 8\sigma/\pi}]$ , define the boundaries of a quasi-ordered KT phase. The transition along the upper curve is similar to the KT transition of the pure system except that the transition temperature and the value of the jump of the exponent  $\eta$  at the transition are reduced by the randomness. The second transition line has no counterpart in the pure case and it signals the reentrance of the disordered phase at low temperature. It occurs because of the presence of a term in the renormalization-group flow equations [1] that makes the vortex fugacity grow continuously

with increasing length scale at low temperature. The effect of a finite vortex-core energy is to push the two transitions down to lower temperatures,  $T_{KT}(\sigma) < T_+(\sigma)$ ,  $T_r(\sigma) < T_-(\sigma)$ .

So far, the reentrant phase has not been seen either in numerical simulations [7,8] or experiments [9] on disordered arrays of Josephson junctions. Although finite-size [7] or pinning [9] effects can account for the failure to observe the reentrance transition, it has been recently suggested [10,11] that, in fact, the latter does not exist. The physical argument supporting this claim is that topological defects can appear at  $T = 0$  only if the energy cost to create them is balanced by an energy gain coming from the random field. However, a simple probabilistic estimate [10] shows that, in an infinite system, the probability of finding sites on which it pays to create an isolated vortex vanishes below  $\sigma_c$ . On the basis of this reasoning one expects the quasi-ordered phase to be stable below the critical disorder at  $T = 0$ . Refining this heuristic considerations by taking into account the interactions between defects, Natterman *et al.* [11] have derived a set of renormalization group equations that reduce to those derived earlier [1] above a crossover temperature  $T^* \approx 2J\sigma$ , but are different from them below it. In the modified theory, vortices are irrelevant in the whole region  $\sigma < \sigma_c$ ,  $T < T_{KT}(\sigma)$ , where the correlation functions exhibit power-law decay. At  $T = 0$  they find a disordered-driven transition at  $\sigma = \sigma_c$  at which there is a jump of the correlation function exponent from a finite value to zero with  $\Delta\eta_c = 1/16$ . Above  $\sigma_c$  the correlation length is finite.

In this paper we present the results of extensive Monte Carlo simulations of the  $XY$  model with random phases. The main difference between our simulations and those performed previously [7,8] resides in the use of finite-size scaling in the analysis of the results. Considerations of scale invariance and universality provide a sensitive tool to distinguish and characterize the different possible phases by imposing stringent conditions on the form of the correlation functions as functions temperature, randomness, and system-size.

Scaling behaviour in the paramagnetic phase, near the KT transition, is most conveniently discussed in terms of the Binder function [16], essentially a ratio of moments of the order parameter. Parametrizing the correlation length in the KT form,  $\xi(T) \sim$

$\exp A/\sqrt{T/T_{KT}-1}$ , and adjusting  $A$  and  $T_{KT}$  so that scaling holds, we determined the  $\sigma$ -dependence of the KT transition temperature and of the expected [1] reentrant transition temperature. We found that  $T_{KT}(\sigma)$  vanishes sharply at  $\sigma_c = \pi/8$ , in agreement with a prediction of Ozeki and Nishimori [12]. The measured disorder-dependence of  $T_{KT}$  near the critical disorder is consistent with the expression that can be derived from the modified renormalization group equations [11]. We found no trace of the expected signature (cf. Section II A) of a reentrant transition in the size dependence of the Binder function at low temperatures.

For  $T \leq T_{KT}$ , analysis of the size-dependence of the moments of the order parameter gives access to the temperature dependence of the correlation function exponent,  $\eta(T, \sigma)$ . It can be shown that, in the case of a reentrant transition,  $d\eta/dT$  must change sign going from positive near  $T_{KT}$  to negative near  $T_r$ . We found instead that  $\eta(T)$  is monotonic and asymptotically approaches the spinwave result [11]  $\eta(T) \sim \frac{1}{2\pi}(T/J + \sigma)$  at low temperature. This suggests that the quasi-ordered phase is stable down to  $T = 0$  for sufficiently weak disorder.

A scaling analysis of the type described above is not possible above  $\sigma_c$  because in this region the disorder and temperature dependence of the correlation length is not known *a priori*. However, from the analysis of the data in the weak-disorder region one can determine not only the critical temperature and exponents but also the full shape of the scaling function. Since by universality the latter is the same throughout the paramagnetic region, we can use it to analyze the results for  $\sigma \geq \sigma_c$  as well. We found that in the strong disorder region the spin-spin correlation function decays exponentially at all temperatures. The correlation length decreases with increasing  $T$  and stays finite as  $T \rightarrow 0$ . The extrapolation of our results to  $T = 0$  is consistent with the form  $\log \xi(T = 0, \sigma) \sim (\sigma - \sigma_c)^{-1}$  expected near a disorder-driven vortex-unbinding transition [11].

## II. METHOD

In this Section we describe the technique and the method of data analysis that we have used in our simulations.

### A. Scaling Analysis.

The analysis is based on the finite-size scaling properties of the moments of the order parameter,

$$q^{(n)} = \left[ \left\langle \left( \frac{1}{N} \sum_{i=1}^N \cos \theta_i \right)^n \right\rangle \right]_d, \quad (3)$$

where  $N = L^2$  is the total number of spins in the system and  $L$  is its linear dimension. Here the symbol  $\langle \dots \rangle$  indicates the usual thermodynamic average with the Gibbs measure,  $P \sim \exp(-\beta H)$ , and  $[\dots]_d$  is the average over the phase shift distribution given in Eq. 2.

In a finite system all configurations related by a global spin rotation enter in the thermodynamic average with equal weight. Since the average over the global rotation angle of all odd moments vanishes, the first non-trivial moments are  $q^{(2)}$  and  $q^{(4)}$ . If  $L \gg a$  ( $a$  is the lattice spacing), we may write

$$\begin{aligned} q^{(2)}(L, T, \sigma) &= L^{-2} \int_{\mathcal{S}} d^2 r \, C_2(r), \\ q^{(4)}(L, T, \sigma) &= L^{-6} \int_{\mathcal{S}} d^2 r_1 d^2 r_2 d^2 r_3 \, C_4(r_1, r_2, r_3), \end{aligned} \quad (4)$$

where the integrals are over the surface of the system and  $C_n$ ,  $n = 2, 4$ , are the two and four-point correlation functions respectively. These are given by the rotationally invariant expressions

$$\begin{aligned} C_2(r) &= \frac{1}{2} [\langle \cos[\theta(\vec{r}) - \theta(0)] \rangle]_d, \\ C_4(\vec{r}_1, \vec{r}_2, \vec{r}_3) &= \frac{3}{8} [\langle \cos[\theta(\vec{r}_1) - \theta(\vec{r}_2) + \theta(\vec{r}_3) - \theta(0)] \rangle]_d. \end{aligned} \quad (5)$$

The scaling theory of phase transitions may be used to determine the general form of the moments as functions of temperature, randomness and system size. In the paramagnetic

phase, sufficiently close to  $T_{KT}$  for the system to be in the scaling regime, the two-point function scales as [16]

$$C_2(\vec{r}) \sim r^{-\eta} \tilde{C}_2(r/\xi), \quad (6)$$

where  $\eta$  is the correlation function exponent,  $\xi \equiv \xi(\sigma, T)$  is the correlation length, and the function  $\tilde{C}_2(x)$  is universal. Using Eq. 6 and the corresponding expression for the four-point function,  $q^{(2)}$  and  $q^{(4)}$  may be written in the form :

$$\begin{aligned} q^{(2)}(L, T, \sigma) &= L^{-\eta} Q_+^{(2)}(L/\xi), \\ q^{(4)}(L, T, \sigma) &= L^{-2\eta} Q_+^{(4)}(L/\xi), \end{aligned} \quad (7)$$

valid in the disordered phase. The functions  $Q_+^{(2)}$  and  $Q_+^{(4)}$  in the expressions above are universal functions of their argument.

The correlation length diverges at  $T_{KT}$  and stays infinite throughout the KT phase. In this phase the long-wavelength behavior of the system is described by renormalized spin-wave theory. The two and four-point functions may be easily calculated within this theory resulting in the expressions :

$$\begin{aligned} C_2(r) &\sim r^{-\eta}, \\ C_4(\vec{r}_1, \vec{r}_2, \vec{r}_3) &\sim \left[ \frac{r_2}{r_1} \frac{|\vec{r}_1 - \vec{r}_3|}{|\vec{r}_1 - \vec{r}_2|} \frac{1}{|\vec{r}_2 - \vec{r}_3|} \right]^\eta. \end{aligned} \quad (8)$$

Substituting Eq. 8 into Eq. 4 we obtain the scaling form of the moments in the quasi-ordered KT phase :

$$\begin{aligned} q^{(2)}(r, T, \sigma) &\sim L^{-\eta} Q_-^{(2)}(\eta), \\ q^{(4)}(r, T, \sigma) &\sim L^{-2\eta} Q_-^{(4)}(\eta), \end{aligned} \quad (9)$$

where the universal functions  $Q_-^{(2)}$  and  $Q_-^{(4)}$ , given by

$$\begin{aligned} Q_-^{(2)}(\eta) &\sim \int d^2x |x|^{-\eta}, \\ Q_-^{(4)}(\eta) &= \int d^2x_1 d^2x_2 d^2x_3 \left[ \frac{x_2}{x_1} \frac{|\vec{x}_1 - \vec{x}_3|}{|\vec{x}_1 - \vec{x}_2|} \frac{1}{|\vec{x}_2 - \vec{x}_3|} \right]^\eta, \end{aligned} \quad (10)$$

depend on temperature and disorder only through the correlation function exponent  $\eta$ .

In the first step of the analysis the unknown factor  $L^{-\eta}$  can be eliminated from Eqs. 7 and 9 by working with the ratio  $u(L, T) = q^{(4)}/[q^{(2)}]^2$ . It is customary to normalize this quantity so that it vanishes at high temperature and it goes to unity for a homogeneous ferromagnet at  $T = 0$ . The normalized quantity, known as the Binder function [16], is defined by

$$g(L, T) = \frac{2}{3}(3 - u(L, T)), \quad (11)$$

It follows from Eqs. 7 and 9 that the Binder function obeys the scaling law

$$g(L, T, \sigma) = \begin{cases} G_+(L/\xi) & , T \geq T_{KT}, \\ G_-(\eta) & , T \leq T_{KT}, \end{cases} \quad (12)$$

where  $G_{\pm}$  are the universal scaling functions in the paramagnetic and quasi-ordered phases, respectively. Our discussion in the Section below is based on the following consequences of Eq. 12 :

1. In the paramagnetic phase  $g(L, T)$  depends on both temperature and system size. However, by choosing  $\xi(T, \sigma)$  appropriately one can make all the data collapse on a universal function,  $G_+(L/\xi)$ .
2. At the KT transition temperature and in the KT phase  $\xi$  is infinite. Therefore the curves for different sizes must merge at  $T_{KT}$ . In the KT phase the Binder function depends on temperature and disorder through a universal function of the correlation function exponent,  $G_-(\eta)$ .
3. A logarithmic plot of  $q^{(2k)}(L, T)$  as a function of  $L$  for different temperatures in the  $KT$  phase must give a series of straight lines whose common slope is  $-k\eta$ .
4. If a reentrant transition occurs, the curves  $g(L, T)$  for the different sizes must split again at  $T_r$  and remain distinct down to  $T \rightarrow 0$ .

In addition, one can show (see Section III A 2) that, if there is a reentrant transition, the slope  $d\eta/dT$  must change sign at some temperature between  $T_{KT}$  and  $T_r$ . This gives yet another signature of reentrance.

## B. Numerical method

We have determined by Monte Carlo simulation the 2–nd and 4–th moments of the order parameter for systems of planar spins on an  $L \times L$  square lattice with periodic boundary conditions. In studies of disordered systems it is particularly crucial to check that thermal equilibrium has been achieved before making the Monte Carlo measurements. We have done this using a procedure first introduced by Bhatt et Young [14] for Ising glasses and generalized by Ray and Moore [15] to the case of  $XY$  spin glasses. The method is based on the comparison between two quantities. One is the mean-square-averaged overlap (MSAO) of two time-delayed configurations of the same evolving system. The other one is the MSAO between the instantaneous configurations of two identical copies (or replicas) of the system that have evolved independently starting from arbitrary initial conditions. The two overlaps [15] are defined by

$$\mathcal{O}(t + t_w, t_w) = \left[ \left\langle \left[ \frac{1}{N} \sum_i \cos [\theta_i(t + t_w) - \theta_i(t_w)] \right]^2 \right\rangle_d \right], \quad (13)$$

and

$$\mathcal{O}_r(t_w) = \left[ \left\langle \left[ \frac{1}{N} \sum_i \cos [\theta_i^{(a)}(t_w) - \theta_i^{(b)}(t_w)] \right]^2 \right\rangle_d \right], \quad (14)$$

respectively. Here,  $t_w$  is a waiting time during which the systems considered here have evolved from the initial conditions, and  $t$  and  $(a)$  and  $(b)$  denote the time delay and the replicas referred to above. Let  $t_{eq}$  and  $t_r$  be the equilibration time and the equilibrium relaxation time, respectively. It follows from general considerations of ergodicity that  $\mathcal{O}(t + t_w, t_w) \rightarrow \mathcal{O}_r(t_w)$  when  $t_w > t_{eq}$  and  $t > t_r$ .

In Monte Carlo simulations thermal averages are replaced by time averages. Thus, to compute the time-delayed overlap the system is simulated for  $t_w$  Monte Carlo time-steps per spin (MCS). The final configuration is stored, and the system is left to evolve further during  $t$  MCS. Measurements are taken at times  $t_m = t + t_w + m$ ,  $m = 0, \dots, M$ , and the required overlap is computed as the average of the overlaps between the configurations at times  $t_m$  and  $t_w$ . Since, in general,  $t_{eq} \gg t_r$ , we may take  $t = t_w$  and write [15] :



$$\mathcal{O}(2t_w, t_w) \sim \left[ \frac{1}{M} \sum_{m=1}^M \left[ \frac{1}{N} \sum_i \cos [\theta_i(2t_w + m) - \theta_i(t_w)] \right]^2 \right]_d. \quad (15)$$

Similarly, in order to compute  $\mathcal{O}_r(t_w)$ , we simulate in parallel two copies of the system for  $t_w$  MCS steps and we take the average of the overlaps of the next  $M$  configurations of the two replicas,

$$\mathcal{O}_r(t_w) \sim \left[ \frac{1}{M} \sum_{m=1}^M \left[ \frac{1}{N} \sum_i \cos [\theta_i^{(a)}(t_w + m) - \theta_i^{(b)}(t_w + m)] \right]^2 \right]_d. \quad (16)$$

In this work we have studied systems with  $L = 4, 6, 8, 10, 12$  and  $16$  for sixteen values of  $\sigma$  in the range  $0 \leq \sigma \leq 1$  and temperatures in the range  $0.3 \leq T/J \leq 1.7$ . For certain values of the disorder and for sizes  $L \leq 10$  we pushed the simulations down to  $T/J = 0.1$ . The thermalization times vary between  $t_w = 2 \times 10^3$  for the smaller systems up to  $t_w = 2 \times 10^5$  for the larger ones at low  $T$ . In all our simulations  $M = t_w$ . The number of realizations of the random bonds simulated to perform the configuration average varies from 256 for the  $16 \times 16$  systems up to 2048 for the smallest ones. However, for values of  $\sigma \sim \sigma_c$  we have averaged over four times as much bond configurations. Our simulations were performed on a 128-processor CRAY T3D parallel computer.

### III. RESULTS

#### A. Weak disorder

We show in Figs. 2a to 2d the numerical values of the Binder function, Eq. 11, as a function of temperature and system-size for four values of  $\sigma$ , representative of our results below  $\sigma_c \approx 0.393$ . The four curves are qualitatively similar except that the temperature scale shifts to the left with increasing disorder. For each size we can identify two regimes. At high temperatures  $g(L, T)$  decreases with increasing temperature or system-size. There is an inflection point (not always seen in the temperature range shown in the figures) and, for sufficiently high  $T$ ,  $g(L, T)$  reaches a temperature-independent plateau whose height depends on the system-size. At low temperatures  $g(L, T)$  is a convex function of  $T$ . Below a certain

temperature the Binder function is  $L$ -independent within the statistical error. There is no further splitting of the curves at low  $T$  in the temperature range covered by our simulations.

These data follow closely the scenario anticipated in the paragraph below Eq. 12 for a system that goes from a disordered to a quasi-ordered state through a Kosterlitz-Thouless transition at a temperature  $T_{KT}$ . The latter is identified as that at which the curves for different sizes merge. The observed absence of size-dependence of  $g$  at low temperatures indicates that the domain of stability of the quasi-ordered phase extends, at least, down to the lowest temperatures that we simulated. It will be seen below that, except for the lowest concentrations, these are below the expected [1] reentrance temperature. The quantitative analysis of the data is as follows.

### 1. The paramagnetic region

To discuss quantitatively the data in the high temperature region we assume that for each value of  $\sigma$  the correlation length is of the KT form,

$$\xi(T) \sim \exp A/\sqrt{T/T_{KT} - 1}, \quad (17)$$

where  $A$  and  $T/T_{KT}$  are disorder-dependent constants. These are determined such that for each  $\sigma$  data for all temperatures and sizes collapse into a unique function of  $L/\xi$  as required by Eq. 12. Examples of the resulting scaling plots for  $g(L, T)$  are shown in Fig. 3 for the same values of  $\sigma$  as in Fig. 2. It may be seen from the figure that the Binder function is a decreasing function of  $L/\xi$ . It decays exponentially for  $L \gg \xi$  and it varies linearly for  $L/\xi \sim 0$ . At the transition temperature  $g$  takes the universal value  $g(L, T_{KT}) = 0.972 \pm 0.001$ . It will be seen below that the differences between the curves corresponding to the different values of  $\sigma$  can be absorbed in a disorder-dependent amplitude in the correlation length, Eq. 17.

The dependence of the critical temperature on randomness obtained from the scaling analysis is shown in Fig. 4. For weak disorder  $T_{KT}$  decreases slowly as a function of  $\sigma$ . When the transition temperature goes below  $T^*$  its variation with  $\sigma$  becomes steeper and

it seems to be very abrupt for  $\sigma \approx \sigma_c$ . In particular, whereas the system has a relatively high transition temperature for  $\sigma = 0.392$ , the analysis of the shape of the Binder function (see below) shows that the  $T = 0$  correlation length is finite for  $\sigma = 0.393$ . The observed sharpness of the transition line agrees with the prediction of Ozeki and Nishimori [12] that, if a low temperature KT phase exists in this model, the phase boundary must be parallel to the temperature axis as  $T \rightarrow 0$ . It may be shown [13] that the modified RG equations of Natterman *et al.* [11] imply that, for  $\sigma \approx \sigma_c$ ,  $T_{KT}(\sigma) \approx 2E_c / \ln [\pi^3 / (\sigma_c - \sigma)]$  where  $E_c$  is the vortex-core energy. We see from Fig. 4 that our results are consistent with this expression.

As a comparison of Figs. 4 and 1 shows,  $T_{KT}$  is much reduced from its upper limit  $T_+$ . This is an indication that the vortex-core energy is relatively small and may considerably renormalize the expected value of the reentrant transition temperature. The core energies can be computed from the measured  $T_{KT}$  by integrating the renormalization group equations of Rubinstein *et al.* [1] along the critical trajectory. The RG equations are :

$$\begin{aligned}\frac{dK}{dl} &= -4\pi^3 K^2 y^2, \\ \frac{dy}{dl} &= (2 - \pi K + \pi K^2 \sigma) y,\end{aligned}\tag{18}$$

where  $K = J/T$  is the running coupling constant and  $y$  is the vortex fugacity whose bare value is related to the temperature and  $E_c$  by  $y_0(T) = \exp(-E_c/T)$ . The renormalization group trajectories, obtained by integration of Eq. 18, are given by the family of curves

$$y^2 = \frac{1}{2\pi^3} (2/K + \pi \ln K - \pi \sigma K) + C,\tag{19}$$

where  $C$  is an integration constant. The critical trajectory is determined by the condition that points on it flow to the fixed point  $y = 0, K = J/T_+$  with  $T_+ = \frac{\pi J}{4} [1 + \sqrt{1 - 8\sigma/\pi}]$ . The physical initial condition intersects the critical trajectory at two temperatures,  $T_{KT}$  and  $T_r$ , solutions of :

$$\exp(-2E_c/T) = \frac{1}{2\pi^3} \left[ 2(K^{-1} - K_+^{-1}) + \pi \ln \frac{K}{K_+} - \pi \sigma (K - K_+) \right].\tag{20}$$

The vortex-core energy  $E_c$  may be determined by substituting the measured values of the KT transition temperature in Eq. 20. We found that  $E_c$  is a decreasing function of disorder

that varies between  $2.28J$  for  $\sigma = 0$  and  $1.9J$  for  $\sigma_c$ . Once the vortex-core energy is known the reentrance temperature may easily be computed by searching for the second solution of Eq. 20. The result is shown by the open circles in Fig. 4. It may be seen that, for  $\sigma \geq 0.25$ ,  $T_r$  lies above the lowest measured temperatures. The fact that the Binder function shows no measurable size-dependence below  $T_r$  for those values of  $\sigma$  for which the region  $T < T_r$  is accessible to us suggests that for sufficiently weak disorder the KT phase is stable at low temperature. The measurements of the disorder and temperature dependence of the exponent  $\eta$  that we present below give further support to this conclusion.

## 2. The quasi-ordered phase

The results in the KT phase below  $T_{KT}$  are most conveniently analyzed in terms of the scaling properties of the moments of the order parameter, Eqs. 9 and 10. Although all even moments contain the same information, we have worked with  $q^{(4)}$  because its temperature dependence is particularly simple. This is shown in Fig. 5 where we plot raw data obtained for  $\sigma = 0.25$ . We see that  $q^{(4)}$  is a decreasing function of temperature and system size that can be quite accurately fitted by a straight line in the temperature range of the simulations. According to Eq. 9 we expect that all the  $L$ -dependence of  $q^{(4)}$  be contained in the prefactor,  $L^{-\eta}$ . The unknown  $\eta$ -dependence in the function  $Q_-^{(4)}(\eta)$  may be eliminated from the problem by making plots of  $\log q^{(4)}$  vs.  $\log L$  for different values of the temperature and of the disorder. For a fixed value of  $\sigma$  we obtain a series of straight lines, one for each temperature, whose slopes are  $-2\eta$ . This is illustrated in Fig. 6, where we represent the data for  $\sigma = 0.25$  as a function of  $L$ .

We determined by this procedure the  $T$ -dependence of  $\eta$  for all values of  $\sigma$ . Results are plotted in Fig. 7 for a few values of the disorder parameter. The correlation function exponent increases continuously with temperature. The extrapolation of our results down to  $T = 0$  is consistent with the spinwave result,  $\eta(T, \sigma) = (T/J + \sigma)/(2\pi)$ . The correlation function exponent at the transition,  $\eta(T_{KT})$ , is disorder-dependent and smaller than  $1/4$ ,

the value for the pure system. The two sets of RG equations [1,11] give different predictions for  $\eta_c$ . However, up to  $\sigma = 0.39$  the difference between the two theories is within our error bars and we can not decide in favour of one or the other.

The curves shown in Fig. 7 are inconsistent with the existence of the reentrant phase. Since all points on the critical trajectory flow to the same fixed point, the value of the correlation function exponent at criticality must be the same at  $T_r$  and at  $T_{KT}$ . This implies that, if there is a reentrant transition,  $d\eta/dT$  must change sign at some temperature intermediate between  $T_{KT}$  and  $T_r$ . Our data in the region  $\sigma \geq 0.25$  where temperatures below  $T_r$  are accessible do not show this behaviour.

### B. Strong disorder.

The Binder function for four values of  $\sigma > \sigma_c$  is shown in Figs. 8a to 8d. The behavior of  $g(L, T)$  in these cases is very different from that shown in Fig. 2 for weak disorder. The Binder functions for different sizes do not collapse but they stay distinct down to the lowest temperatures considered. Although it is obviously impossible to guarantee that they do not join at lower temperatures, this seems unlikely because, in order to merge, the curves would have to turn upwards at low temperatures. However, in all the cases in which we did observe a KT transition,  $g(L, T)$  was found to be a convex function of  $T$  at low temperature. We interpret this behavior as evidence that for  $\sigma \geq \sigma_c$  the correlation length stays finite at all temperatures.

For a fixed size,  $g(L, T)$  saturates to a constant value with decreasing  $T$  indicating that, at low temperature, the correlation length only depends on the strength of the disorder. This dependence is very strong as shown in Fig. 9 where we represent the temperature and  $\sigma$  dependence of  $g(L, T)$  for  $L = 16$ , our largest size, and  $T/J \geq 0.3$ . There is a five-fold decrease in the asymptotic value  $g(L, T)$  when  $\sigma$  varies between 0.4 and 1.

In order to analyze our results quantitatively it is convenient to fit them to a simple analytic expression. We have chosen a four-parameter function,

$$g(L, T) = m_1 + m_2 [1 - \tanh[m_3(T - T_0)]] , \quad (21)$$

that, despite its simplicity, accurately describes all the data throughout the paramagnetic phase as the solid lines in Figs. 8 and 9 show. Thanks to this parameterization our results can easily be extrapolated down to  $T = 0$ .

The scaling analysis of the data in Figs. 8a to 8d can not be performed in the same way as for  $\sigma \leq \sigma_c$  because we do not have here an explicit expression giving the temperature dependence of the correlation length. However, this is not actually necessary. By universality, the scaling function  $G_+(x)$  of Eq. 12 is the same throughout the disordered phase. If we determine it from the data in the weak-disorder region, we can use it in the region  $\sigma \geq \sigma_c$  too.

In order to do this we reconsider the scaling plots of Fig. 3. The reason why the curves for different values of  $\sigma$  are all different is that in the scaling analysis the correlation length has been determined up to an amplitude that depends on the strength of the disorder. We can compute all but one of the amplitudes by rescaling horizontally the curves of Fig. 3 such that they can all be superimposed to one of them. Choosing the curve for  $\sigma = 0$  as reference and its amplitude as the unit of length, this procedure leads to the universal scaling function shown in Fig. 10. This plot where there more than six hundred points corresponding to different system sizes, temperatures and values of  $\sigma$  lie on the same master curve is a beautiful example of universality.

Having thus determined the scaling function  $G_+(x)$ , the correlation length in the strong-disorder regime can be computed by reading from Fig. 10 the values of  $L/\xi$  corresponding to the measured values of  $g(L, T)$ . This yields the temperature and disorder-dependent correlation length except for an undetermined scale factor. The results of the analysis are presented in Fig. 11. At high temperature the correlation length is small and varies slowly with disorder. At low temperatures  $\xi$  is  $T$ -independent and reaches a saturation value that increases very fast as we approach the critical disorder from the right. As seen in the figure, the error bars become very large when  $\sigma \rightarrow \sigma_c$ , the uncertainties in  $G_+$  (cf. Fig. 10) and

in the value of the Binder function leading to large errors in  $\xi$  for  $L/\xi \ll 1$ . The results can be reliably extrapolated to  $T = 0$  only for  $\sigma \geq 0.49$ . The disorder dependence of the ground-state correlation length in this region of values of  $\sigma$  is represented in Fig. 12. It can be seen that the data are well described by the expression  $\xi(T = 0, \sigma) \sim \exp[b/(1 - \sigma_c/\sigma)]$  that follows from the  $T = 0$  form of the modified RG equations of Natterman *et al.* [11]. This result supports their conclusion that at zero-temperature there is a disorder-driven transition at  $\sigma_c$  between two spin-glass states that differ by the properties of the spin-spin correlation function.

In summary, we have studied the two-dimensional  $XY$  model with random phases by Monte Carlo simulation. An essential element in our work is the use of finite-size scaling in the analysis of the results. The scaling properties of the moments of the order parameter do not show the characteristic signatures that should be present if of a low-temperature reentrant transition occurred. Our results suggest that renormalized spinwave theory is applicable as  $T \rightarrow 0$  for sufficiently weak disorder. This is inconsistent with theories that predict the reentrance of the paramagnetic phase at low temperature [1] but agrees with more recent theories [10,11].

## REFERENCES

- [1] M. Rubinstein, B. Shraiman, and D. R. Nelson, Phys. Rev. B **27**, 1800 (1983).
- [2] M.-C. Cha, and H. A. Fertig, Phys. Rev. Lett. **73**, 870 (1994).
- [3] E. Granato, and J. M. Kosterlitz, Phys. Rev. B **33**, 6533 (1986).
- [4] E. Granato, and J. M. Kosterlitz, Phys. Rev. Lett. **62**, 823 (1989).
- [5] M. P. A. Fisher, T. A. Tokuyasu, and A. P. Young, Phys. Rev. Lett. **66**, 2931 (1991).
- [6] J. M. Kosterlitz, and D. J. Thouless, J. Phys. C **6**, 1181 (1973).
- [7] M. G. Forrester, S. P. Benz, and C. J. Lobb, Phys. Rev. B **41**, 8749 (1989).
- [8] Amitabha Chakrabarti, and Chandan Dasgupta, Phys. Rev. B **37**, 7557 (1988).
- [9] M. G. Forrester, Hu Jong Lee, M. Tinkham, and C. J. Lobb, Phys. Rev. B **37**, 5966 (1988).
- [10] M.-C. Cha, and H. A. Fertig, Phys. Rev. Lett. **74**, 4867 (1995).
- [11] T. Natterman, S. Scheidl, S. E. Korshunov, and M. S. Li, J. Phys. I (France) **5**, 565 (1995).
- [12] Y. Ozeki, and H. Nishimori, J. Phys. A **26**, 3399 (1993).
- [13] J. Maucourt, and D. R. Grempel, unpublished.
- [14] R. N. Bhatt, and A. P. Young, Phys. Rev. B **37**, 5606 (1988).
- [15] P. Ray, and M. A. Moore, Phys. Rev. B **45**, 5361 (1992).
- [16] K. Binder, Z. Phys. B **43**, 119 (1981)



## FIGURES

FIG. 1. Schematic phase diagram of the  $XY$  model with random phases in the  $T - \sigma$  plane according to the theory of Rubinstein *et al.*.  $T_+$  and  $T_-$  are, respectively, the values of the KT transition temperature and of the reentrance temperature for the case of an infinite vortex core energy.

FIG. 2. The Binder function as a function of temperature for different system sizes and several values of the strength of the disorder in the weak disorder regime. (a)  $\sigma = 0.09$ , (b)  $\sigma = 0.16$ , (c)  $\sigma = 0.25$ , and (d)  $\sigma = 0.36$ .

FIG. 3. A scaling plot of the data presented in the previous figure. For each value of  $\sigma$  the data for all system-sizes and temperatures collapse into a single function of  $L/\xi(T, \sigma)$ .

FIG. 4. The Kosterlitz-Thouless transition temperature as a function of disorder as determined from the scaling plots. The dotted line is the prediction of the modified RG equations. The temperatures at which reentrance was expected to occur are indicated by the open circles.

FIG. 5. The fourth moment of the order-parameter as a function of temperature for  $\sigma = 0.25$  and several system sizes.

FIG. 6. Logarithmic plot of the fourth moment of the order-parameter as a function of system-size for  $\sigma = 0.25$  and several temperatures. The latter go between  $0.1J$  and  $0.7J$  in steps of  $0.05J$ . The top curve corresponds to the lowest temperature.

FIG. 7. The correlation function exponent as a function of temperature for several values of  $\sigma$ .

FIG. 8. The Binder function as a function of temperature for different system sizes and several values of the strength of the disorder in the strong disorder regime. (a)  $\sigma = 0.49$ , (b)  $\sigma = 0.64$ , (c)  $\sigma = 0.81$ , and (d)  $\sigma = 1$ . The solid lines are fits to the functional form described in the text.

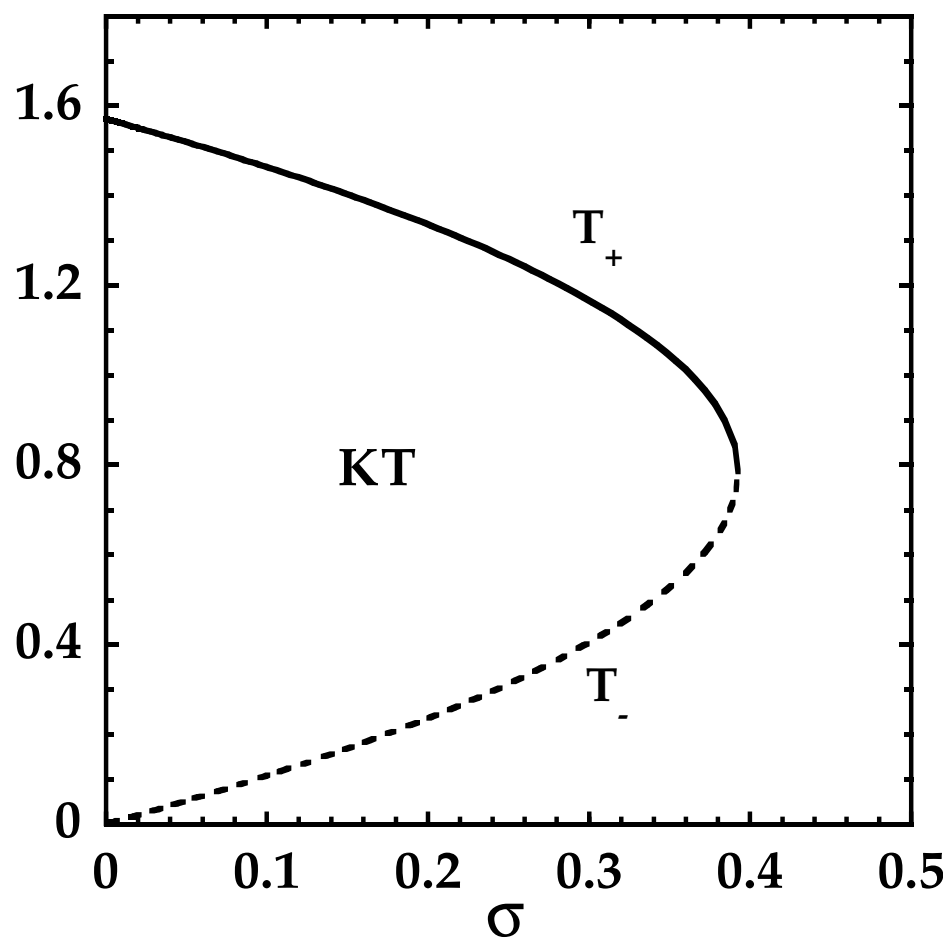
FIG. 9. The Binder function as a function of temperature and disorder for several values of the strength of the disorder and  $L = 16$ .

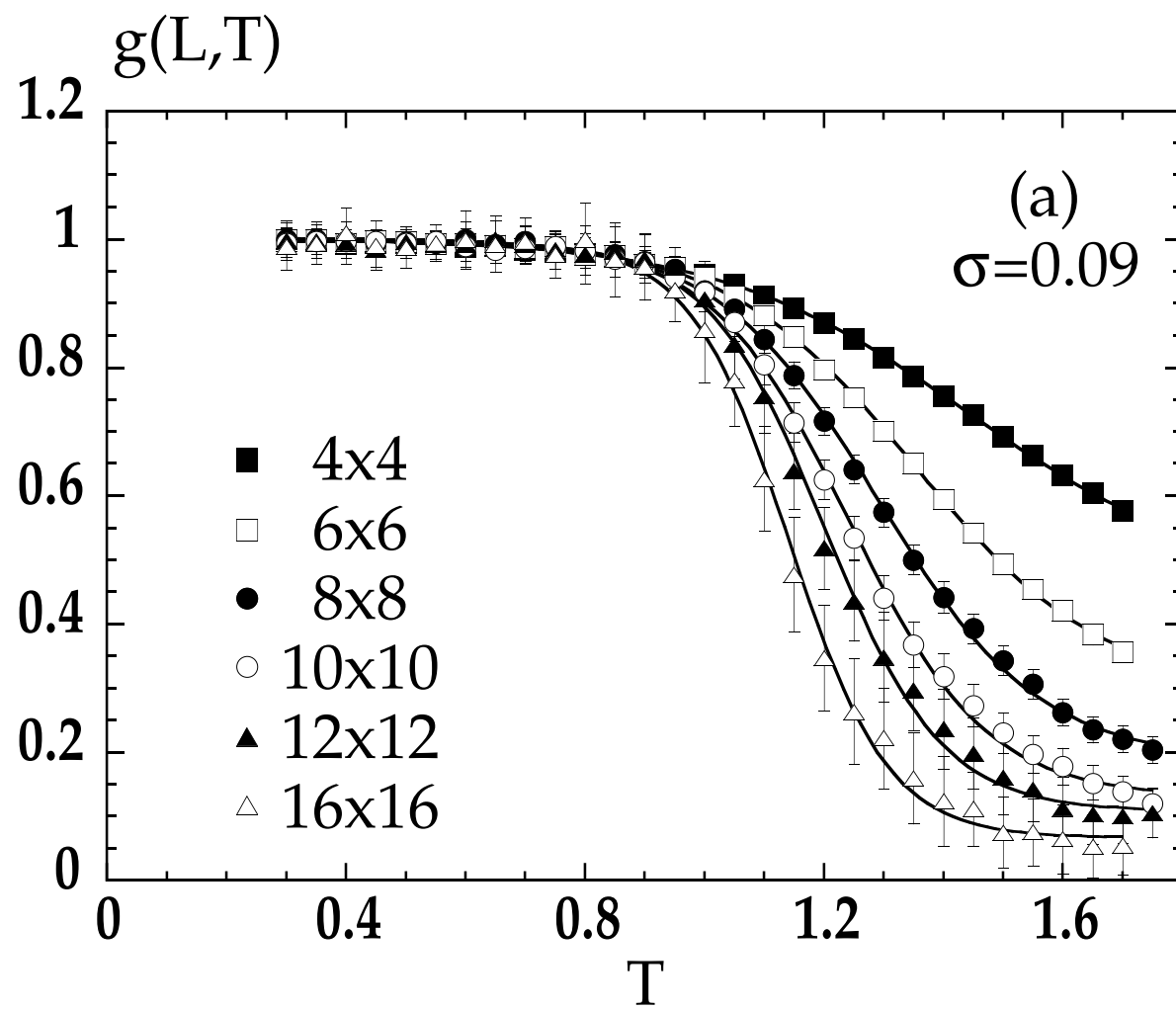
FIG. 10. The universal scaling function in the disordered phase as a function of  $x = L/\xi$ .

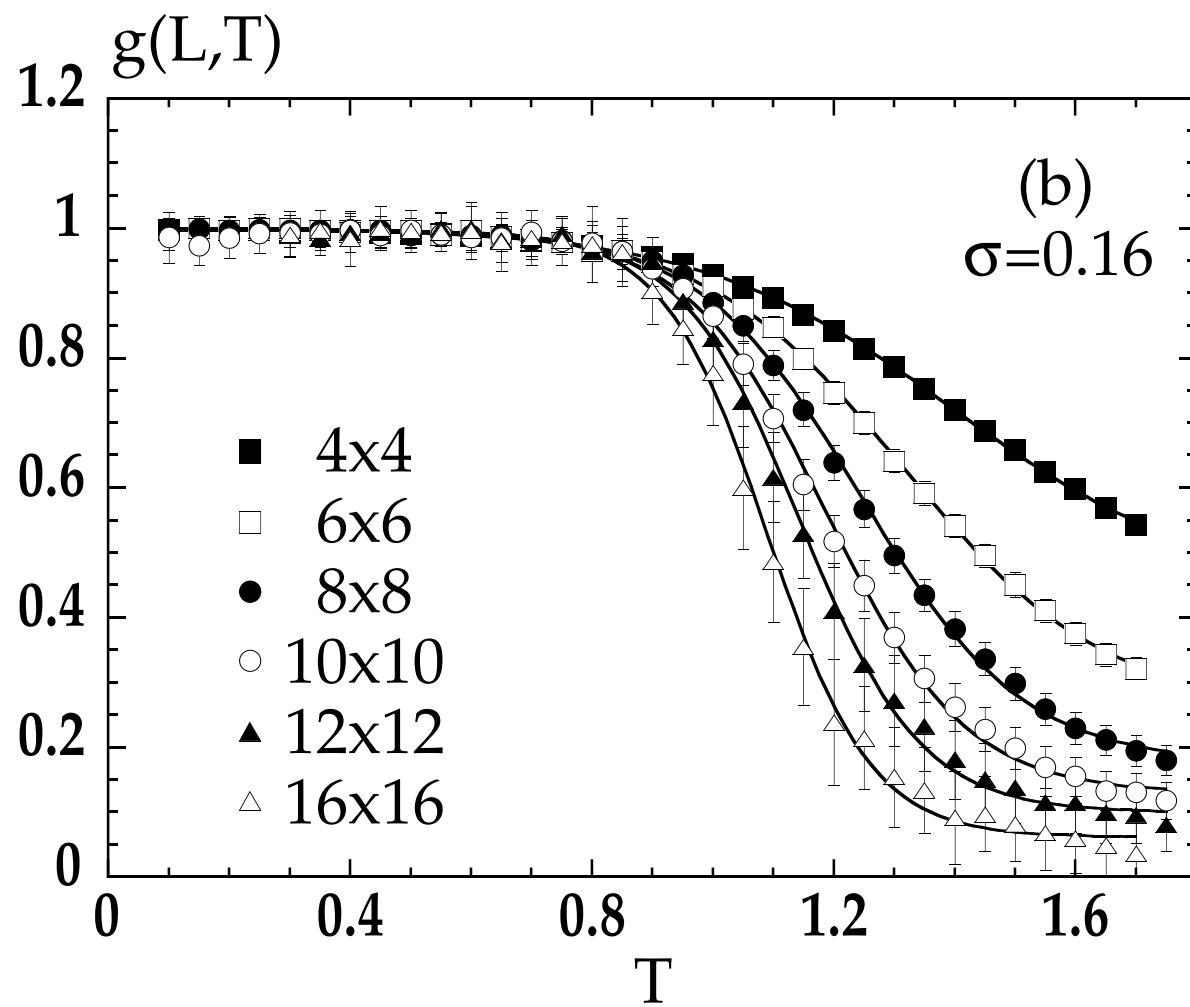
FIG. 11. Temperature dependence of the correlation length (in arbitrary units) in the strong disorder regime for the same values of  $\sigma$  as in Fig. 9. The highest curve corresponds to the lowest value of the disorder. The full lines are derived from the fits in Fig. 8.

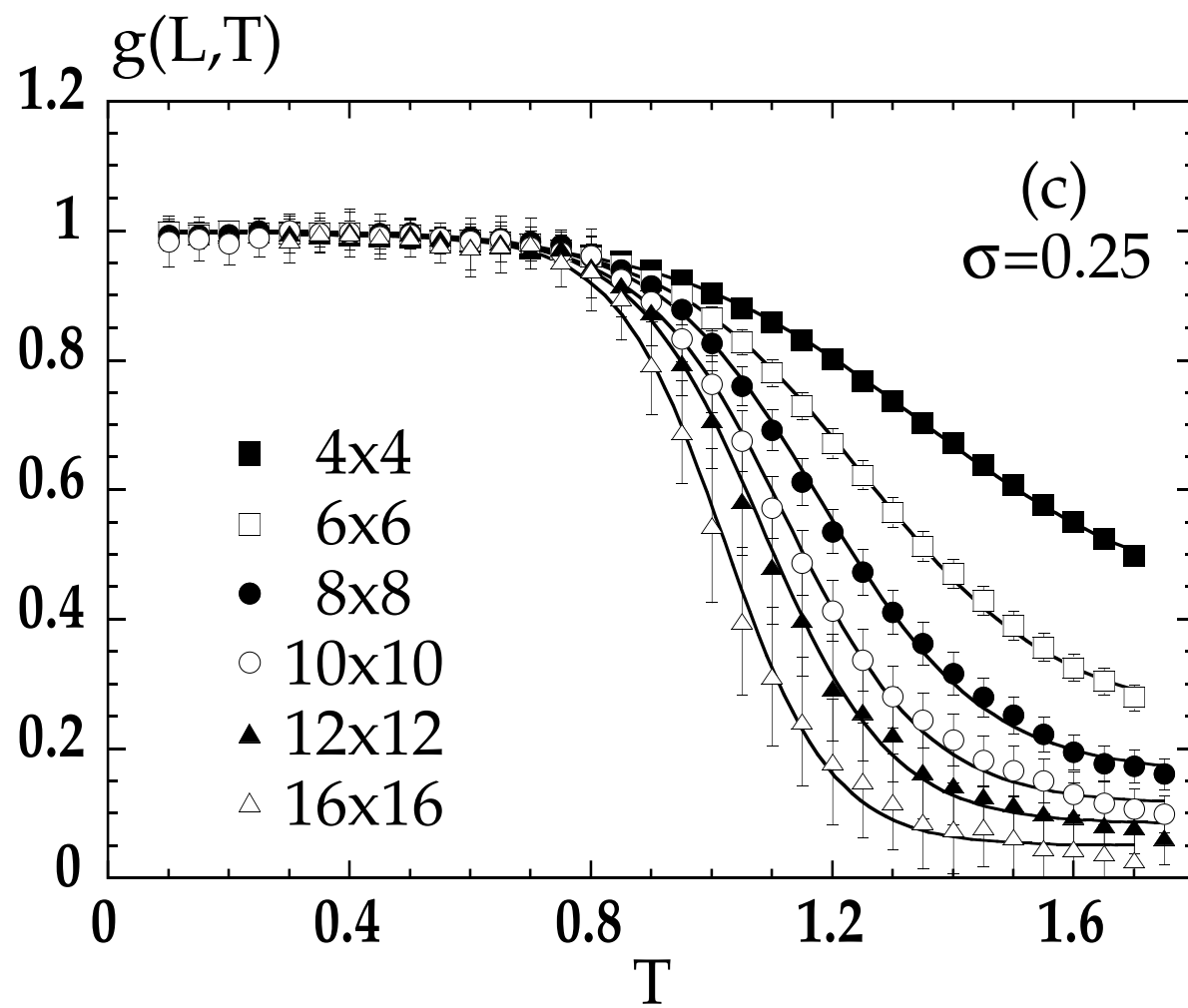
FIG. 12. The zero-temperature correlation length as a function of disorder. The unit of length is arbitrary. The solid line is a fit to the expression  $\xi \sim \exp[b/(\sigma_c - \sigma)]$  with  $b = 0.69$ . The divergence at  $\sigma_c$  signals the disorder-driven unbinding of vortices.

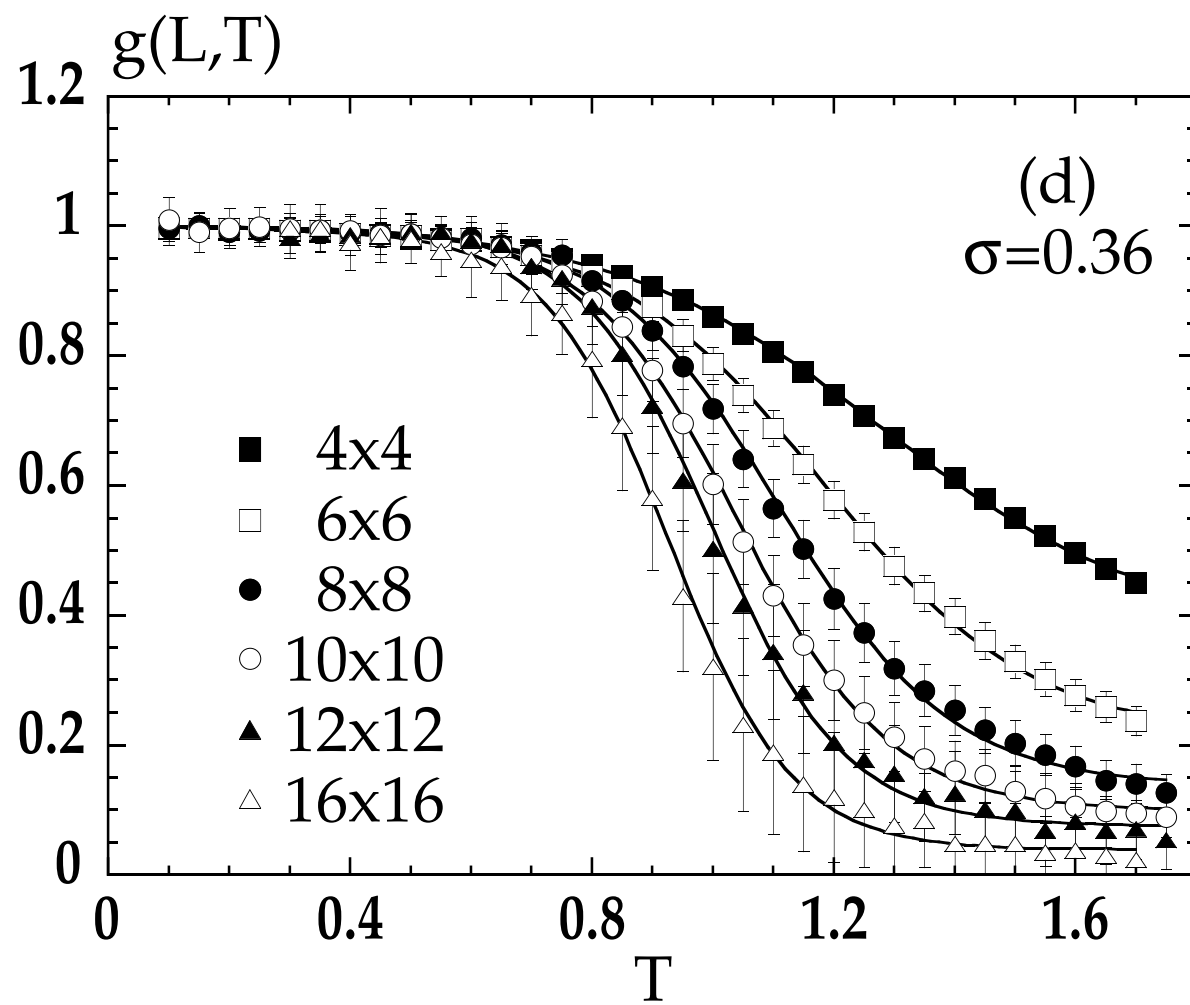
$T / J$

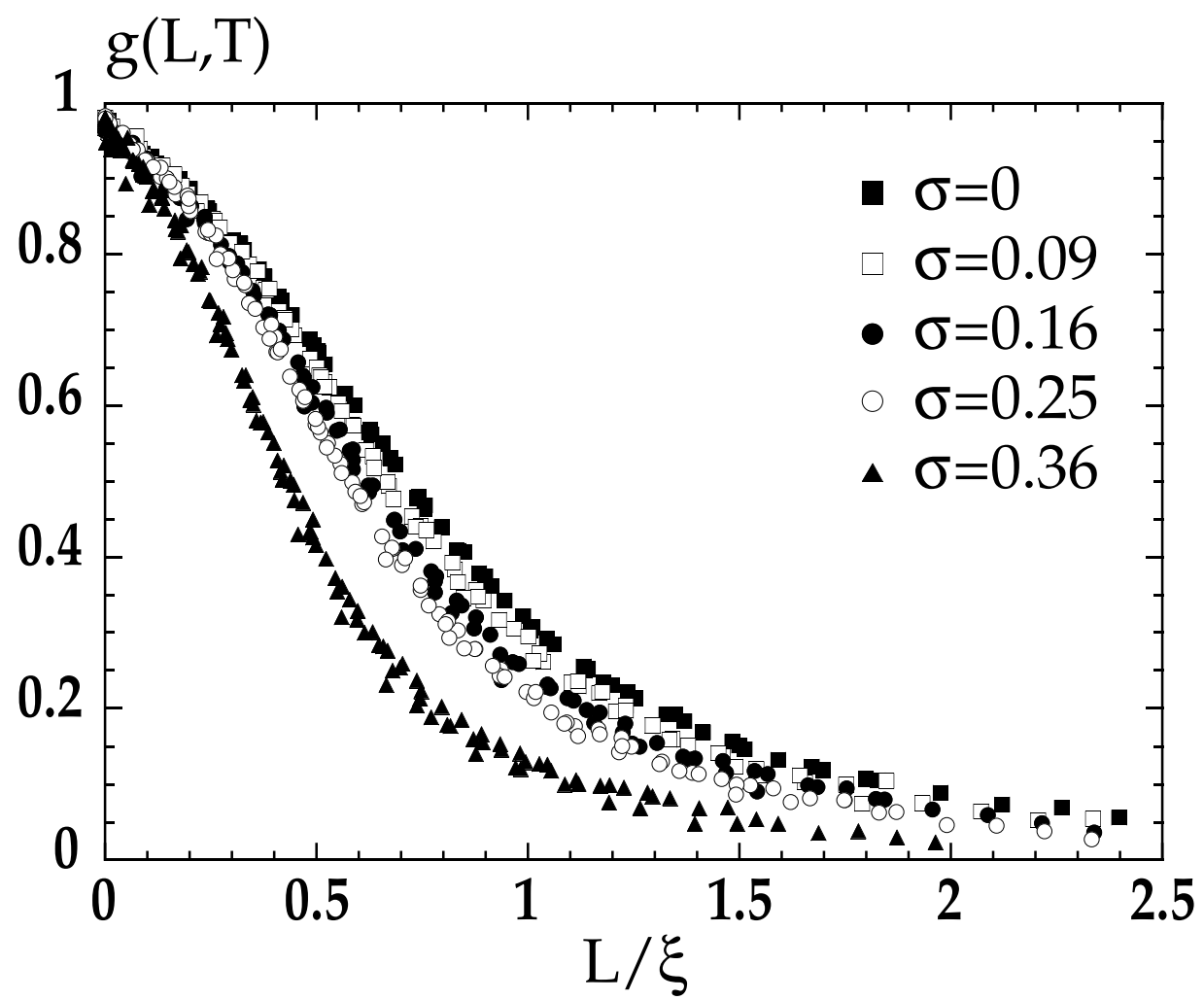














$T_{KT} / J$

